Outer and Central Charged Residues in DIVS4 of Skeletal Muscle Sodium Channels Have Differing Roles in Deactivation

James Groome,*† Esther Fujimoto,† Lisa Walter,* and Peter Ruben†
*Department of Biology, Harvey Mudd College, Claremont, California 91711; and †Department of Biology, Utah State University, Logan, Utah 84322-5305 USA

ABSTRACT We tested the effects of charge-neutralizing mutations of the eight arginine residues in DIVS4 of the rat skeletal muscle sodium channel ($rNa_V1.4$) on deactivation gating from the open and inactivated states. We hypothesized that neutralization of outer or central charges would accelerate the I-to-C transition as measured by recovery delay because these represent a portion of the immobilizable charge. R1Q abbreviated recovery delay as a consequence of reduced charge content. R4Q increased delay, whereas R5Q abbreviated delay, and charge-substitutions at these residues indicated that each effect was allosteric. We also hypothesized that neutralization of any residue in DIVS4 would slow the O-to-C transition with reduction in positive charge. Reduction in charge at R1, and to a lesser extent at R5, slowed open-state deactivation, while charge neutralizations at R2, R3, R4, R6, and R7 accelerated open-state deactivation. Our findings suggest that arginine residues in DIVS4 in $rNa_V1.4$ have differing roles in channel closure from open and inactivated states. Furthermore, they suggest that deactivation in DIVS4 is regulated by charge interaction between the electrical field with the outermost residue, and by local allosteric interactions imparted by central charges.

INTRODUCTION

Voltage-sensitive Na^+ channels are responsible for the upstroke of the action potential in excitable cells (Hodgkin and Huxley, 1952; Keynes and Meves, 1993). Depolarization of the membrane potential promotes a transient increase in sodium permeability (activation), which is followed by rapid inactivation (Aldrich et al., 1983). The amino acid sequence of the sodium channel α-subunit predicts four homologous domains containing six transmembrane segments (Noda et al., 1984). The fourth segment (S4) in each domain contains positively charged residues, and several lines of experimentation suggest a role for sodium channel S4 segments as voltage sensors during activation (Stühmer et al., 1989; Yang and Horn, 1995; Yang et al., 1996; Horn et al., 2000).

Unlike tetrameric potassium channels with identical charge content in S4 segments, sodium channel S4 segments possess unequal charge content. For example, in skeletal muscle sodium channels, DIVS4 contains charged residues at each turn of the proposed α helix (Trimmer et al, 1989). Previous studies have revealed that charged residues within the S4 segments may have domain-specific roles. For example, outer arginine residues in DIVS4 couple activation to fast inactivation (Chahine et al., 1994; Chen et al., 1996; Kontis and Goldin, 1997; Sheets et al., 1999; Horn et al., 2000) and central arginine and neutral residues in this voltage sensor play a role in slow inactivation (Mitrovic et al., 2000).

In sodium channels, a tripeptide IFM motif in the cytoplasmic linker between DIII and DIV is an important component of fast inactivation (Vassilev et al., 1988; West et al., 1992; Kellenberger et al., 1996; Horn et al., 2000). Fast inactivation is accompanied by immobilization of gating charge (Armstrong and Bezanilla, 1977). Immobilization of voltage sensors in DIII and DIV limits recovery from fast inactivation, such that the rate of recovery from fast inactivation is paralleled by recovery of immobilized charge (Cha et al., 1999; Kühn and Greef, 1999; Sheets et al., 1999, 2000). The outermost arginine residue (R1) and two central arginine residues (R4 and R5) in DIVS4 compose at least a portion of immobilizable charge (Ruben et al., 1999; Kühn and Greef, 1999; Sheets et al., 1999) and may contribute to a domain-specific role of DIVS4 in fast inactivation.

Inactivated sodium channels must deactivate to become available for activation, with a voltage-sensitive delay before recovery from fast inactivation (Kuo and Bean, 1994). Limited transition through the open state has been described only in $Na_V1.6$ (Raman and Bean, 2001). In $hNa_V1.4$, the delay in recovery (here called inactivated-state deactivation) is abbreviated by neutralization of the outermost charged residue in DIIIS4 (K1126C) or DIVS4 (R1448C; Ji et al., 1996; Groome et al., 1999). Reduced charge immobilization in R1448C (Ruben et al., 1999) may explain the abbreviation of recovery delay in this mutation, such that charge immobilization and transmembrane voltage are determinants of the rate of deactivation from the fast-inactivated state.

Charge neutralizing mutations of central residues R4 and R5 in DIVS4 affect both charge immobilization and recovery from fast inactivation (Abbruzzese et al., 1998; Kühn and Greef, 1999; Ruben et al., 1999), as does charge neutralization at R1. These data suggested to us that inactivated-state deactivation might be regulated by outer and central

Submitted April 25, 2001, and accepted for publication December 7, 2001.
Address reprint requests to Dr. Peter C. Ruben, Dept. of Biology, Utah State University, Logan, UT 84322-5305. Tel.: 435-797-2136; Fax: 435-797-1575; E-mail: pruben@biology.usu.edu.

0006-3495/02/03/1293/15 $2.00

charged residues in DIVS4, with its high proportion of immobilizable charge.

Sodium channels that are opened by brief depolarization return to a closed state in response to hyperpolarization, here called open-state deactivation. The decay of current in this transition is usually best described by a monoexponential function (Rayner et al., 1993; Ji et al., 1996, Kontis et al., 1997; Featherstone et al., 1998), suggesting that a single S4 translocation to the hyperpolarized-favored position is functionally sufficient for channel closure. Domain-specific roles for S4 segments in open-state deactivation are suggested by the results of studies with charge-neutralizing mutations. For example, the O-to-C transition is accelerated by neutralizations of charged residues in DIS4 or DIIS4 (Kontis and Goldin, 1997; Groome et al., 1999). However, the O-to-C transition is slowed by neutralizations of charged residues in DIIIS4 (Kontis and Goldin, 1997; Groome et al., 1999) or of the outermost charged residue in DIVS4 (Ji et al., 1996; Groome et al., 1999), suggesting that deactivation is limited by charge content in DIII and DIV.

In the present study, we tested the hypotheses that open-state deactivation (regulated by transmembrane electric field) is regulated by similar contributions from each of eight arginine residues in DIVS4, whereas inactivated-state deactivation (regulated by charge immobilization and electric field) is regulated primarily by outer and central residues in this voltage sensor. We find that activation is affected similarly by each of eight charge-neutralizing mutations in DIVS4. In contrast, fast inactivation and deactivation from either the open or inactivated state are differentially affected by these R/Q mutations. Our results suggest that translocations of DIVS4 from the open or inactivated state to a hyperpolarized-favored position are dependent on the electrostatic or allosteric character of charged residues in this voltage sensor. Portions of this work have been reported in abstract form (Groome et al., 2001).

MATERIALS AND METHODS

Site-directed mutagenesis

Mutations were prepared by site-directed mutagenesis using a PCR overlap extension method (Ho et al., 1989). R1C was prepared as previously described (Featherstone et al., 1998). Other PCR fragments were similarly prepared with appropriate oligonucleotides containing the mutation. R1Q, R2Q, R3Q, R4Q, R1K, and R4K fragments were cloned into *Bst*1107I–*Sac*II sites of $rNa_V1.4$/pGH19. R6Q, R7Q, and R8Q fragments were cloned into *Bsr*GI sites. Clones were mapped with restriction enzymes to determine the correct orientation. R5Q and R5K were prepared using a single round of PCR because the *Sac*II site was contained within the mutant primer. Fragments were cloned into *Bst*1017I–*Sac*II sites, and all clones were verified by sequencing.

Oocyte preparation

In vitro transcription of sodium channel α- and β_1-subunits was performed as previously described (Featherstone et al., 1998). mRNA for α- and β_1-subunits (1:1 vol, α-subunit at 1 μg/μl, β_1-subunit at 3 μg/μl) were co-injected (50 nl/oocyte) into *Xenopus laevis* oocytes surgically removed from frogs anesthetized with 0.17% tricaine (3-aminobenzoic acid ethyl ester, Sigma, St. Louis, MO). Oocytes were separated using 2 mg/ml collagenase (Sigma) in a solution containing (in mM): NaCl 96, KCl 2, $MgCl_2$ 20, HEPES 5, pH 7.4. Before recording, oocytes were incubated at 18°C for at least 4 days in culture medium containing (in mM): NaCl 96, KCl 2, $MgCl_2$ 1, $CaCl_2$ 1.8, HEPES 5, sodium pyruvate 2.5, pH 7.4, with 100 mg/l gentamicin and 3% horse serum (Gibco BRL, Rockville, MD). Vitelline membranes were removed immediately before recording, following a 3-min treatment in a hyperosmotic solution containing (in mM): NaCl 96, KCl 2, $MgCl_2$ 20, HEPES 5, mannitol 400, pH 7.4.

Electrophysiology

All recordings were from oocyte membranes using cell-attached macropatch techniques (Featherstone et al., 1998). The pipette solution used was (in mM): NaCl 96, KCl 4, $MgCl_2$ 1, $CaCl_2$ 1.8, HEPES 5, pH 7.4. The bath solution used was (in mM): NaCl 9.6, KCl 88, EGTA 11, HEPES 5, pH 7.4. Voltage clamping and data acquisition were done as previously described (Featherstone et al., 1998) using an EPC-9 patch-clamp amplifier (HEKA, Lambrecht, Germany) controlled via Pulse software (HEKA) running on a Power Macintosh G3. Data were acquired at 5 μs per point and low-pass filtered at 5 kHz during acquisition. Experimental bath temperature was maintained at 15 $\pm$ 0.1°C for all experiments with a Peltier device and HCC-100A temperature controller (Dagan, Minneapolis, MN). Oocyte holding potential was -120 mV to -150 mV, and leak subtraction was automatically performed using a p/4 protocol. Leak and capacitance subtractions were done upon patch formation and corrected before each voltage clamp experiment. Analyses and graphing were done using PulseFit (HEKA) and Igor Pro (Wavemetrics, Lake Oswego, OR).

Conductance/voltage ($g(V)$) relationships were derived using the equation:

$$g_{Na} = I_{max}/(V_M - E_{Na})$$

where g_{Na} is sodium conductance, I_{max} is calculated as the peak test pulse current, V_M is the test pulse voltage, and E_{Na} is the measured sodium equilibrium potential. Steady-state fast inactivation (h_∞) was determined by measuring peak current amplitudes obtained with depolarizing test pulses to -20 mV following variable-voltage, 500-ms conditioning pulses. Current amplitudes were normalized to the maximum peak current amplitude obtained following a prepulse to -150 mV and plotted as a function of prepulse voltage. Activation and steady-state fast inactivation (h_∞) curves were fit by Boltzmann distributions, as:

$$(g/g_{max}) = 1/(1 + \exp(-ze_o(V_M - V_{1/2})/kT))$$

and

$$(I/I_{max}) = 1/(1 + \exp(-ze_0(V_M - V_{1/2})/kT))$$

where V_M is the test pulse or prepulse potential, z is the apparent valence, e_0 is the elementary charge, $V_{1/2}$ is the midpoint voltage, k is the Boltzmann constant, and T is the temperature in Kelvin.

Descriptions of open-state deactivation rates, given as time constants (τ_D), were derived from the monoexponential decay of tail currents according to the function:

$$I(t) = \text{offset} + a_1 \exp(-t/\tau_D)$$

where $I(t)$ is current amplitude as a function of time, offset is the plateau amplitude (asymptote), a_1 is current amplitude at time = 0, and τ_D is the deactivation time constant.

Recovery from fast inactivation was determined using a double pulse protocol (Kuo and Bean, 1994). From a holding potential of -150 mV, a

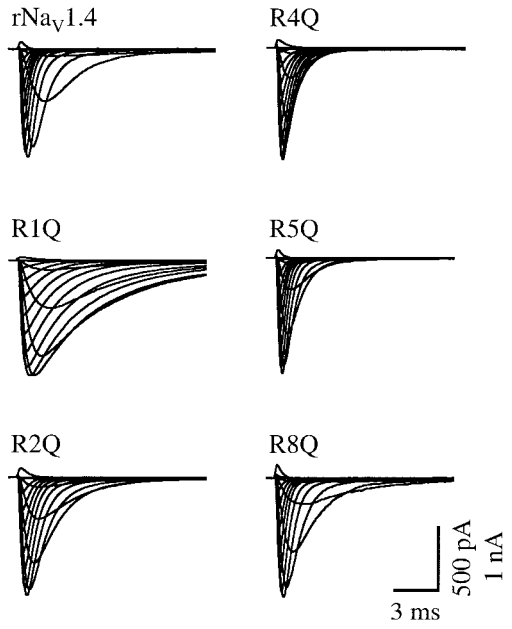

FIGURE 1 Sodium currents in $rNa_V1.4$ and R/Q substitutions in DIVS4. Channels were held at −150 mV before step depolarizations of 20-ms duration over a voltage range from −90 mV to +60 mV; averaged sweeps are shown for $rNa_V1.4$ and charge-neutralizing mutations. Calibration: 3 ms, 500 pA for R1Q and R2Q; 1 nA for others.

21-ms depolarizing voltage step to 0 mV was used to inactivate channels. This was followed by a command to voltages that ranged between −190 mV and −90 mV for durations that ranged from 0.05 ms to 5 ms in steps of 50 μs. For some mutations, interpulse duration was increased to 10 ms at voltages more depolarized than −130 mV to accurately assess slow recovery. The interpulse was followed by a 5-ms recovery test pulse to 0 mV. Recovery current amplitudes from 2 to 5 ms were extrapolated to the time (t) at which current amplitude was zero to determine the delay in onset to recovery from fast inactivation. Recovery rates were calculated as the reciprocal of recovery time constants.

All results are reported as mean ± SEM. Statistical significance was determined using Student's t-test or, in those cases where there was a statistically significant difference between standard deviations, Welch's alternative t-test. Statistical significance of difference was accepted at p values ≤ 0.05. For recovery and deactivation kinetics, t-tests of mutations at individual voltages were used to compare differences over the voltage range tested. Significant differences of mutations for at least three consecutive voltages were taken as an indication of a significant difference in voltage dependence. Statistical comparisons at individual voltages were also noted where significant differences were not continuous over several voltages.

RESULTS

Activation

Effects of R/Q mutations in DIVS4 on activation parameters were determined from $g(V)$ curves derived (see Methods) from peak current amplitudes in response to depolarizing pulses ranging from −90 mV to +60 mV from a holding potential of −150 mV (Figs. 1 and 2). Apparent valence was significantly reduced in all 8 R/Q mutations in DIVS4 from 3.89 in $rNa_V1.4$ (Table 1). Seven of these mutations produced a significantly depolarized shift of the conductance curve as determined from the midpoint of activation ($rNa_V1.4$ = −45.1 mV), with effects of R1Q not quite significant (−42.7 mV, p = 0.052). Time to peak activation, measured during depolarizing test pulses to −20 mV, was significantly increased in R1Q, R2Q, R3Q, and R6Q compared to $rNa_V1.4$ at 637.7 μs. Thus, most activation parameters were similarly affected by reduction in positive charge with each of the R/Q mutations in DIVS4.

Inactivation

Effects of R/Q mutations in DIVS4 on steady-state fast inactivation (h_∞) are summarized in Table 1 and in Fig. 2. The apparent valence of −4.1 in $rNa_V1.4$ was significantly decreased in R1Q, R2Q, and R5Q. The midpoint of the h_∞ curve was significantly left-shifted by R1Q, R2Q, R3Q, R4Q, and R5Q compared to $rNa_V1.4$ at −90.9 mV, with the largest hyperpolarizing shift observed for R4Q. R6Q, R7Q, and R8Q produced a significant right-shift of the midpoint of the h_∞ curve, with the largest depolarizing shift caused by R6Q.

Time constants of open-state fast inactivation (τ_h) were determined from the decay of sodium currents during step depolarizations to potentials ranging from −60 mV to +20 mV (Fig. 3). R1Q and R1C dramatically slowed the rate of fast inactivation compared to $rNa_V1.4$, to an equivalent extent. With the exception of R7Q, each of the charge neutralizations in DIVS4 significantly increased τ_h at 0 mV (Table 1). The voltage dependence of fast inactivation was decreased in R1Q and R5Q, and to a lesser extent in R2–4Q. These findings are consistent with earlier studies indicating an important role for this voltage sensor in fast inactivation (Chen et al., 1996; Kühn and Greef, 1999; Sheets et al., 1999; Horn et al., 2000).

Recovery from the inactivated state

A double-pulse protocol was used to examine the recovery from fast inactivation in $rNa_V1.4$ and R/Q mutations in DIVS4 (Fig. 4). Current decayed completely during the first depolarizing pulse for $rNa_V1.4$ or charge-neutralizing mutations in DIVS4, and we did not observe persistent current in these experiments. Recovery delays of mutations in DIVS4 shown in Fig. 5, and recovery rates shown in Fig. 6, were measured using a monoexponential fit to peak amplitudes of recovering current (see Methods).

Recovery delay was abbreviated, compared to $rNa_V1.4$, by R1Q, R1C, R5Q, and R6Q (Figs. 4 and 5). Recovery delay was also abbreviated by R8Q at some voltages. Recovery delay was longer than $rNa_V1.4$ in R2Q, R3Q, and R4Q. At voltages more positive than −110 mV recovery

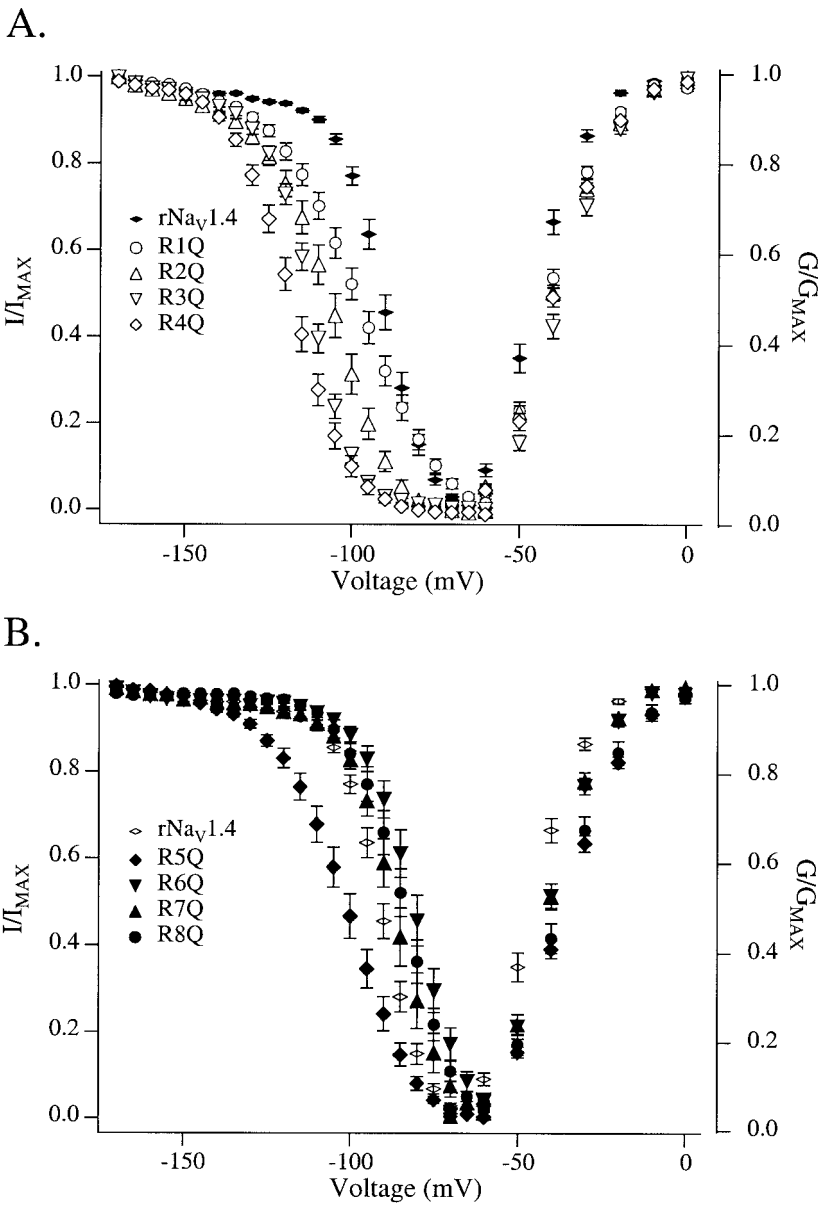

FIGURE 2 Conductance/voltage relationships in $rNa_V1.4$ and R1–4/Q (*open symbols, A*) or R5–8/Q (*closed symbols, B*) mutations in DIVS4. Steady-state fast inactivation (h_∞) curves were generated from experiments in which channels were held for 500-ms prepulses at voltages ranging from −170 mV to −35 mV before a 0 mV depolarizing test pulse. Activation curves were generated from Boltzmann fits of *I/V* relationships in experiments, as shown in Fig. 1. Values represent mean ± SEM; $n = 12–30$.

TABLE 1 Activation and inactivation parameters of $rNa_v1.4$ and charge-neutralizing mutations in DIVS4

Mutation	$g(V_{1/2})$ (mV)	Apparent Valence of Activation	Time to Peak Activation, −20 mV (μs)	τ_h at 0 mV (ms)	$h(V_{1/2})$ (mV)	Apparent Valence of Inactivation
$rNa_v1.4$	−45.1 ± 0.94	3.89 ± 0.10	637.7 ± 21.5	0.39 ± 0.01	−90.9 ± 1.1	−4.09 ± 0.34
R1Q	−42.7 ± 0.79	3.27 ± 0.04*	863.7 ± 34.7*	2.20 ± 0.08*	−98.7 ± 1.7*	−2.28 ± 0.17*
R2Q	−39.5 ± 0.70*	3.11 ± 0.04*	803.5 ± 24.3*	0.72 ± 0.02*	−107.0 ± 1.9*	−3.12 ± 0.08*
R3Q	−37.1 ± 0.86*	3.36 ± 0.06*	770.5 ± 17.6*	0.72 ± 0.02*	−112.4 ± 0.9*	−3.88 ± 0.16
R4Q	−39.3 ± 0.72*	3.34 ± 0.07*	681.5 ± 16.4	0.46 ± 0.01*	−117.8 ± 1.5*	−3.38 ± 0.08
R5Q	−35.1 ± 0.70*	2.85 ± 0.07*	641.0 ± 22.3	0.64 ± 0.03*	−101.5 ± 2.0*	−2.74 ± 0.04*
R6Q	−41.0 ± 1.0*	3.52 ± 0.11*	686.4 ± 10.2*	0.43 ± 0.01*	−81.9 ± 1.8*	−4.09 ± 0.10
R7Q	−40.1 ± 0.92*	3.56 ± 0.05*	690.6 ± 31.2	0.42 ± 0.02	−86.5 ± 1.9*	−4.19 ± 0.11
R8Q	−36.9 ± 1.4*	3.10 ± 0.07*	635.6 ± 28.6	0.43 ± 0.02*	−84.6 ± 1.7*	−3.81 ± 0.10

*Significant difference compared with $rNa_v1.4$ at $p \leq 0.05$.

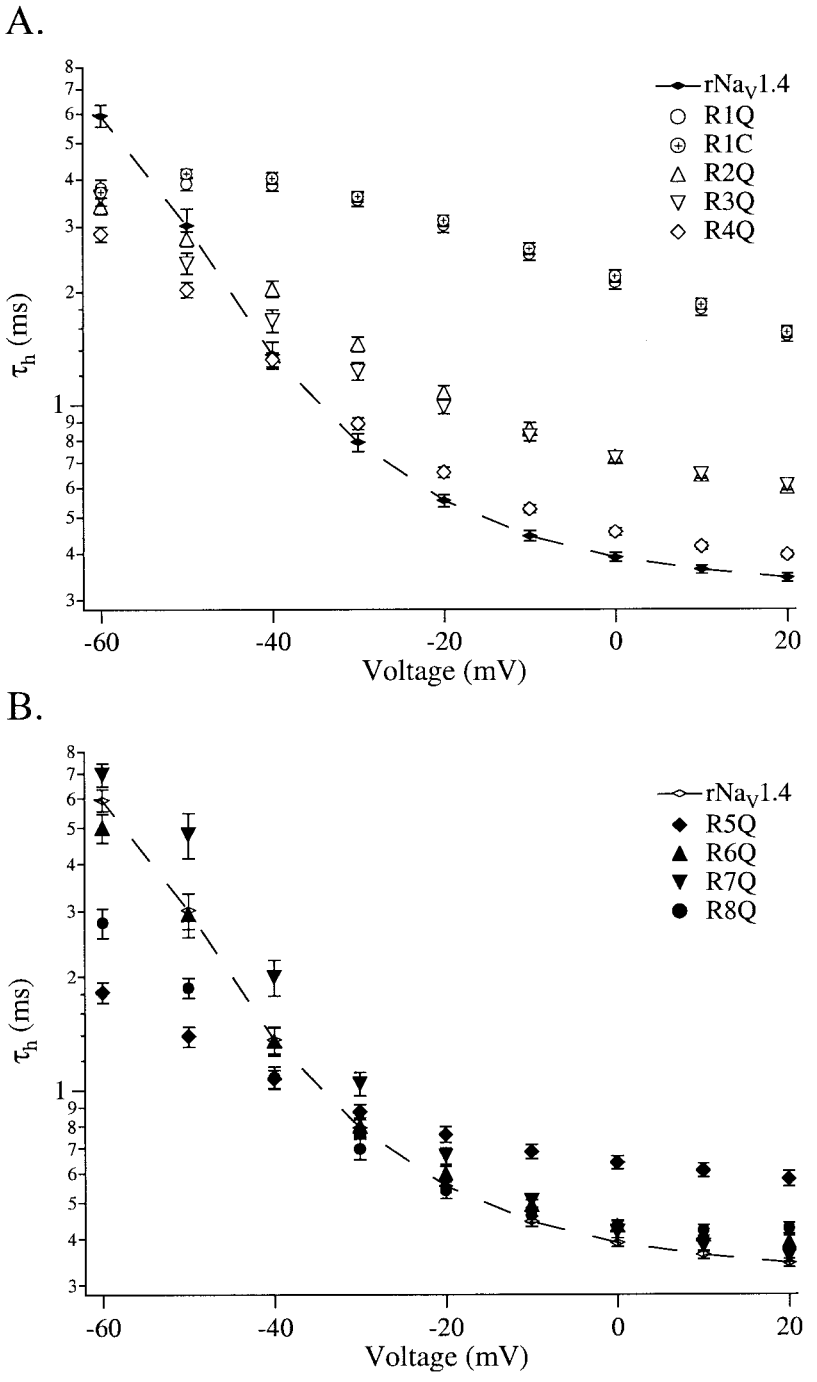

FIGURE 3 Effects of charge neutralizations in DIVS4 on the kinetics of fast inactivation. τ_h values were calculated from the monoexponential decay of current during step depolarizations to potentials ranging from −60 mV to +20 mV, from a holding potential of −150 mV. R1–4/Q mutations are indicated by open symbols (*A*), and R5–8/Q mutations are indicated by closed symbols (*B*). The dotted line is included with $rNa_V1.4$ for clarity. Values represent mean ± SEM; n = 13–30.

was not sufficient after 10 ms to allow a reasonable estimate of recovery delay in R4Q, and delay was not determined at −90 mV in R3Q for the same reason. Recovery rate was, to some extent, predictable from delay measurements such that abbreviated delay correlated with more rapid recovery from fast inactivation, and prolonged delay correlated with slower recovery. Thus, recovery was significantly faster than $rNa_V1.4$ in R1Q, R1C, R5Q, R6Q, and R8Q, whereas recovery was significantly slower than $rNa_V1.4$ in R2Q, R3Q, and R4Q (Figs. 4 and 6).

Open-state deactivation

Channels were opened by steps to 0 mV or 50 mV for durations of 0.25 ms or 0.5 ms, and tail currents were elicited by command hyperpolarizations to voltages ranging from −140 mV to −50 mV. To determine the voltage range over which tail current decay represented deactivation, as opposed to fast inactivation, we used the $rNa_V1.4$ IFM1303QQQ mutation (IFM/QQQ, Featherstone et al., 1998). Command voltages more negative than −60 mV

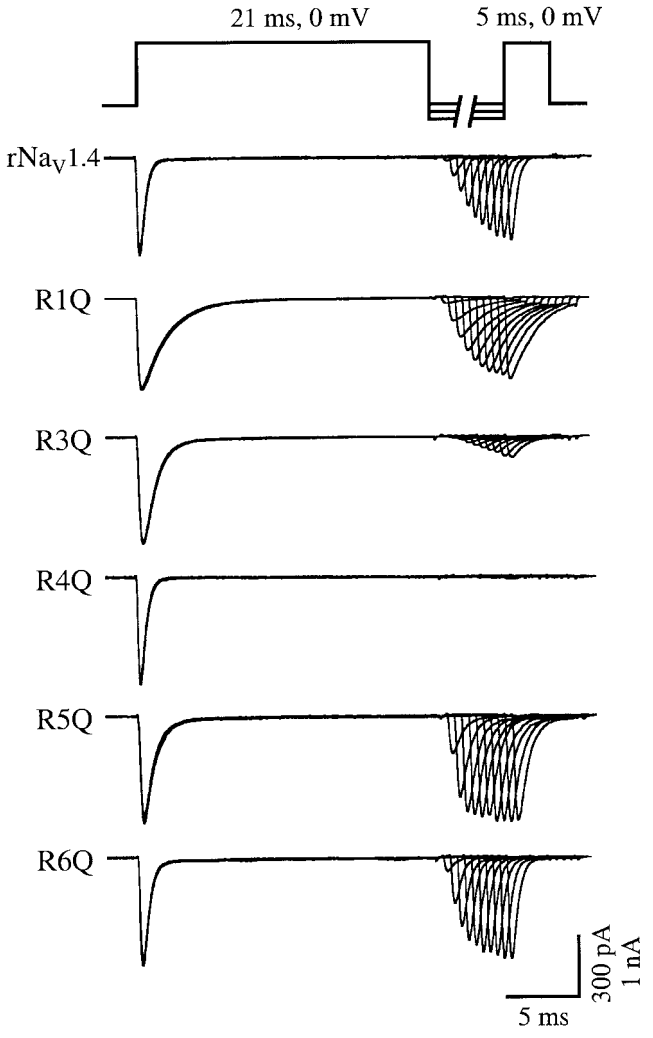

FIGURE 4 Double-pulse protocol used to measure recovery delay and rate in rNa$_V$1.4 and charge-neutralizing mutations DIVS4. For each trace, every 10th sweep of the 21-ms, 0-mV depolarizing pulse used to inactivate channels and the second 5-ms, 0-mV depolarizing pulse used to assess recovery are shown. Calibration: 5 ms, 300 pA for R4Q, R5Q; 1 nA for others.

elicited a complete decay of tail currents with this mutation (Fig. 7 *C*). We therefore measured open-state deactivation at voltages from −140 mV to −70 mV. IFM/QQQ increased τ_D compared to rNa$_V$1.4 over the full voltage range tested. τ_D was increased in rNa$_V$1.4 or IFM/QQQ when more positive or longer depolarizations were used to open channels (Fig. 7, *B* and *D*). The effect of conditioning pulse potential and duration on τ_D was decreased when less negative commands were used to elicit tail currents in rNa$_V$1.4, but was voltage-independent in IFM/QQQ. These findings suggest that the structures that control fast inactivation may have contributed to the decay of tail currents when longer or more positive depolarizations were used to open channels.

We used 0 mV, 0.25-ms depolarizations to open channels followed by commands from −140 mV to −70 mV to measure open-state deactivation in charge neutralizing mutations in DIVS4. Voltage-dependent effects on τ_D of charge-neutralizing mutations are shown for R1–R4 in Fig. 8, and for R5–R8 in Fig. 9. Open-state deactivation was slowed in R1Q and R1C (Fig. 8). In contrast, R2Q and R3Q accelerated deactivation, and R4Q accelerated deactivation at −130 mV, −110 mV, and −100 mV. Deactivation was slowed by R5Q compared to rNa$_V$1.4 at −80 mV and −70 mV (Fig. 9). Deactivation was accelerated by R6Q and R7Q, and was unaffected by R8Q.

For each of the R/Q mutations in DIVS4, we compared the effect of longer duration or more positive depolarizations used to open channels on tail currents elicited with hyperpolarizing commands. To do this, we compared τ_D from protocols in which a 50-mV, 0.5-ms depolarizing pulse was used to open channels, to τ_D obtained with a 0-mV, 0.25-ms protocol. For each macropatch we calculated the ratio of τ_D following a 50-mV, 0.5-ms protocol to τ_D following a 0-mV, 0.25-ms protocol (Fig. 10).

For most mutations, the τ_D ratio showed little voltage dependence at command voltages from −140 mV to −110 mV. At command potentials less negative than −110 mV, the τ_D ratios for rNa$_V$1.4 and mutations of charged residues in DIVS4 were voltage-dependent, whereas the ratios for IFM/QQQ were voltage-independent. The τ_D ratios in IFM/QQQ were consistently higher compared to rNa$_V$1.4 (Fig. 10 *A*).

Charge-neutralizing mutations in DIVS4 differentially affected τ_D ratio. R1Q and R1C decreased τ_D ratios at voltages up to −90 mV (Fig. 10 *B*). τ_D ratios for R2–3Q were similar to rNa$_V$1.4 at most voltages. For central residues, R4Q slightly decreased τ_D ratios at hyperpolarized voltages (Fig. 10 *B*) while R5Q slightly increased τ_D ratios at depolarized voltages (Fig. 10 *C*). τ_D ratios for R6–7Q were greater than rNa$_V$1.4 at most voltages. R8Q, like R4Q, decreased the τ_D ratio at hyperpolarized voltages.

Effects of charge-substituting mutations in DIVS4

We observed that both open-state and inactivated-state deactivation kinetics were differentially affected by R/Q substitutions in DIVS4. Thus, R1Q produced the greatest effect on open-state deactivation, whereas R4Q and R5Q most dramatically altered inactivated-state deactivation. We questioned whether effects on deactivation were a consequence of reduction in charge or alteration in structure, and explored this issue by comparing the effects on deactivation of R/Q and R/K mutations at R1, R4, and R5.

Charge substitution of the outermost arginine (R1K) minimized or reversed the abbreviation of recovery delay produced by R1Q (Fig. 11 *A*). Although recovery delay was significantly longer in R1K than rNa$_V$1.4 at several voltages, recovery delay in R1Q was significantly shorter than R1K at all voltages tested. Recovery rate in R1Q was

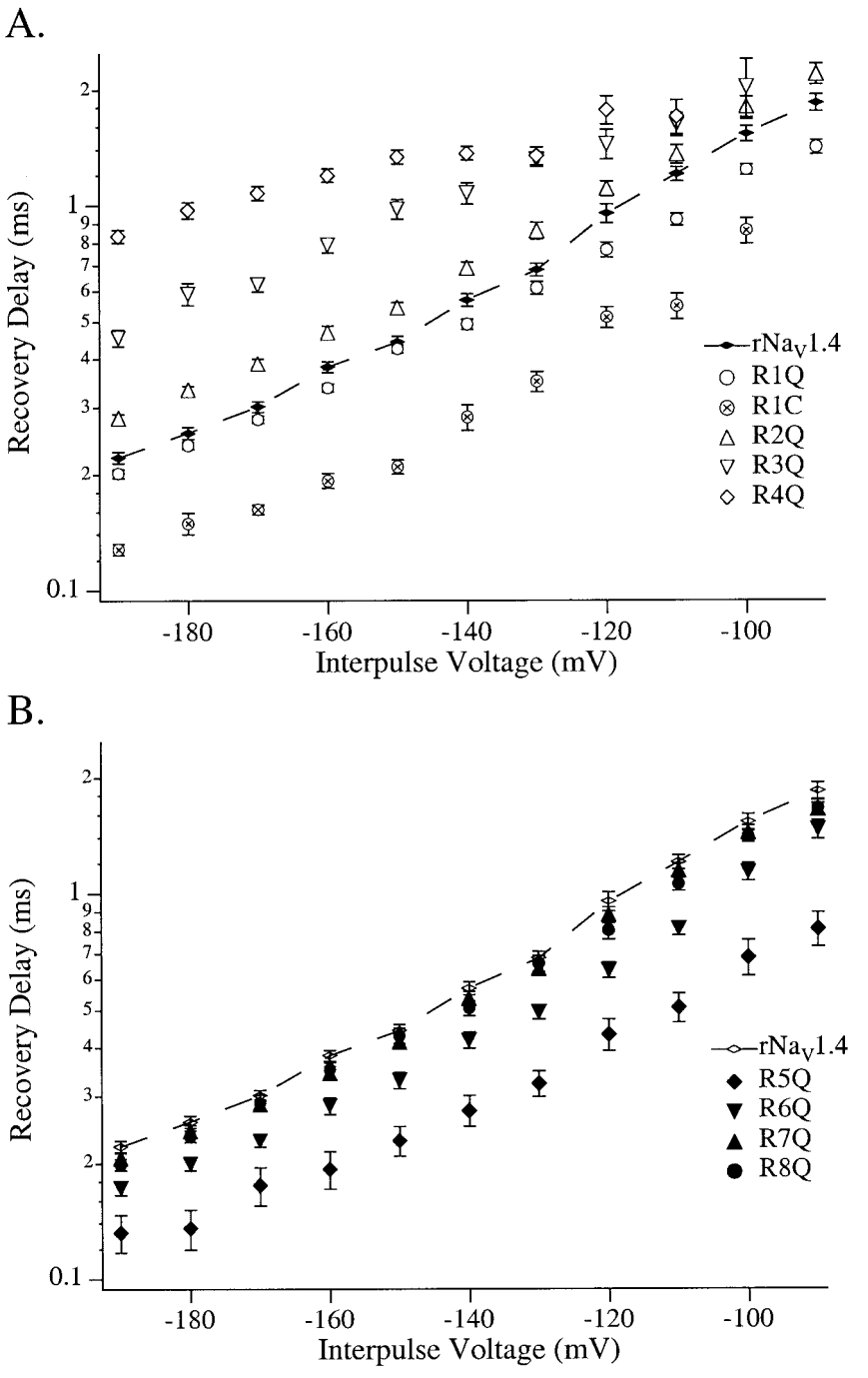

FIGURE 5 Voltage dependence of delay in the onset to recovery from fast inactivation in $rNa_V1.4$ and R/Q mutations in DIVS4 as calculated from the *x*-intercept of a monoexponential fit of recovery current. R1C and R1–4/Q mutations are indicated by open symbols (*A*), and R5–8/Q mutations are indicated by closed symbols (*B*). The dotted line is included with $rNa_V1.4$ for clarity. Values represent mean ± SEM; $n = 12–24$.

increased compared to $rNa_V1.4$, while recovery rate in R1K was statistically similar to $rNa_V1.4$ (Fig. 11 *B*).

Charge substitution at central residues (R4K or R5K) significantly abbreviated delay compared to $rNa_V1.4$ at all voltages tested (Fig. 11 *A*). Thus, R4K abbreviated delay in contrast to the effect of R4Q, whereas R5K abbreviated delay to an extent equivalent to that produced by R5Q. Charge substitution at R4 and R5 produced effects on rate predictable from delay measurements, such that recovery rates were faster in R4K and in R5K than $rNa_V1.4$ (Fig. 11 *B*). These findings suggest that reduction in charge accounted for abbreviated delay in R1Q, whereas allosteric effects accounted for increased delay (R4Q) and for abbreviated delay (R5Q) for mutations at central residues.

Open-state deactivation in R1K was prolonged compared to $rNa_V1.4$ at more depolarized commands, but to a lesser extent than that observed for R1Q (Fig. 12 *A*). R4K slowed open-state deactivation at depolarized commands, in contrast to the effects of R4Q (Fig. 12 *B*). The slight effect of R5Q to increase τ_D compared to $rNa_V1.4$ was reversed in

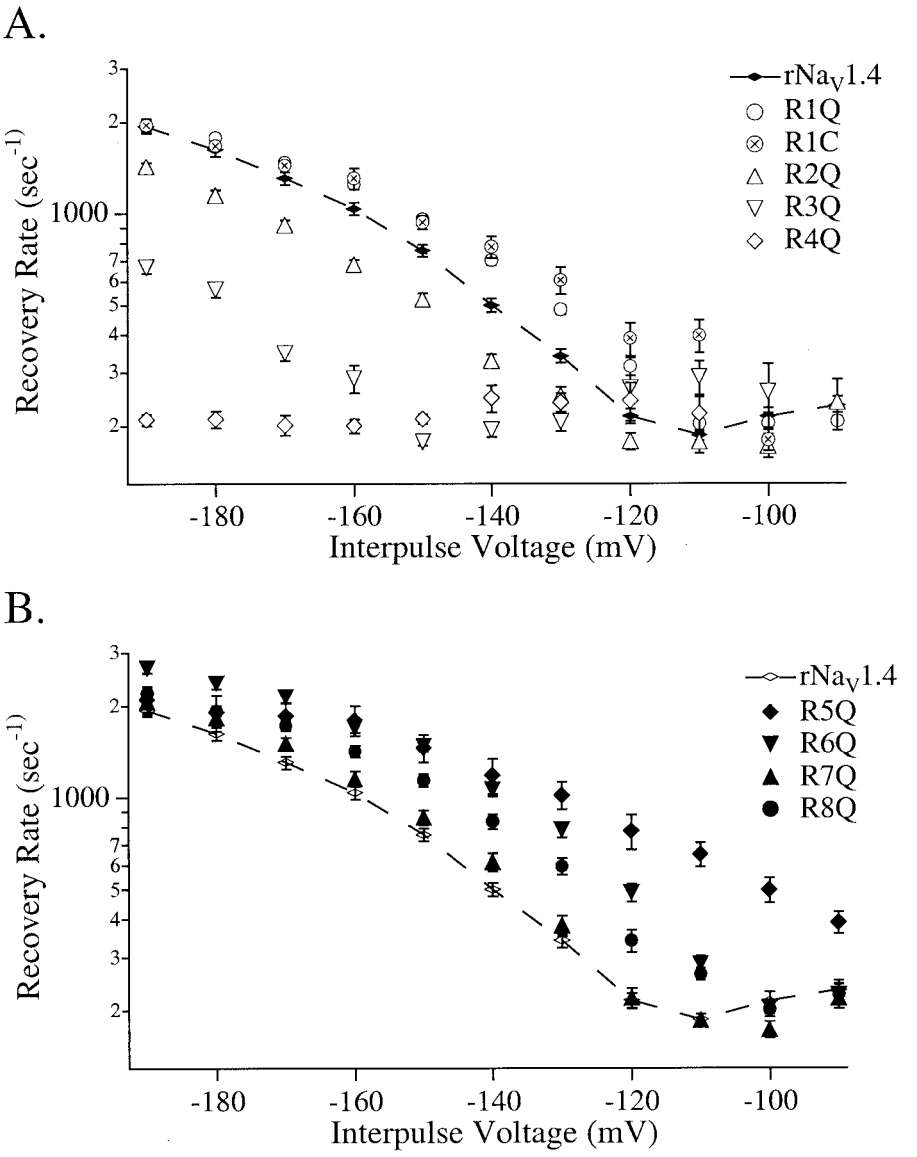

FIGURE 6 Fast inactivation recovery rates measured from the recovery curve. R1C and R1–4/Q mutations are indicated by open symbols (*A*), and R5–8/Q mutations are indicated by closed symbols (*B*). The dotted line is included with rNa$_V$1.4 for clarity. Values represent mean ± SEM; n = 12–24.

R5K (Fig. 12 *C*). These findings suggest that reductions in charge at R1 and R5 were at least in part responsible for slower open-state deactivation in R1Q and R5Q.

DISCUSSION

The putative voltage sensors in sodium channels possess unequal charge content, suggesting that S4 segments may play distinct roles in channel gating. Mutagenesis and accessibility studies have shown that DIVS4 is an important component of the coupling between activation and fast inactivation. In addition, immobilization of charge in DIII and DIV with fast inactivation may limit the return of these voltage sensors in response to hyperpolarization, and thus regulate the I-to-C transition. Gating current measurements have shown that outer and central arginines in DIVS4 compose a portion of the immobilizable charge. These findings motivated our present hypothesis that specific charged residues in DIVS4 regulate deactivation from the inactivated state.

It has also been demonstrated that brief depolarizations are followed, upon hyperpolarization, by tail currents with voltage-dependent monoexponential kinetics. This implies that the O-to-C transition is a one-step process. The most parsimonious explanation for the voltage dependence of this process is that open-state deactivation is accomplished by the translocation of a single voltage sensor to its hyperpolarized favored position. DIVS4 has the highest charge content in any of the four domains. Thus, we focused one aspect of this study on the contribution of each of the charged residues in DIVS4 to open-state deactivation.

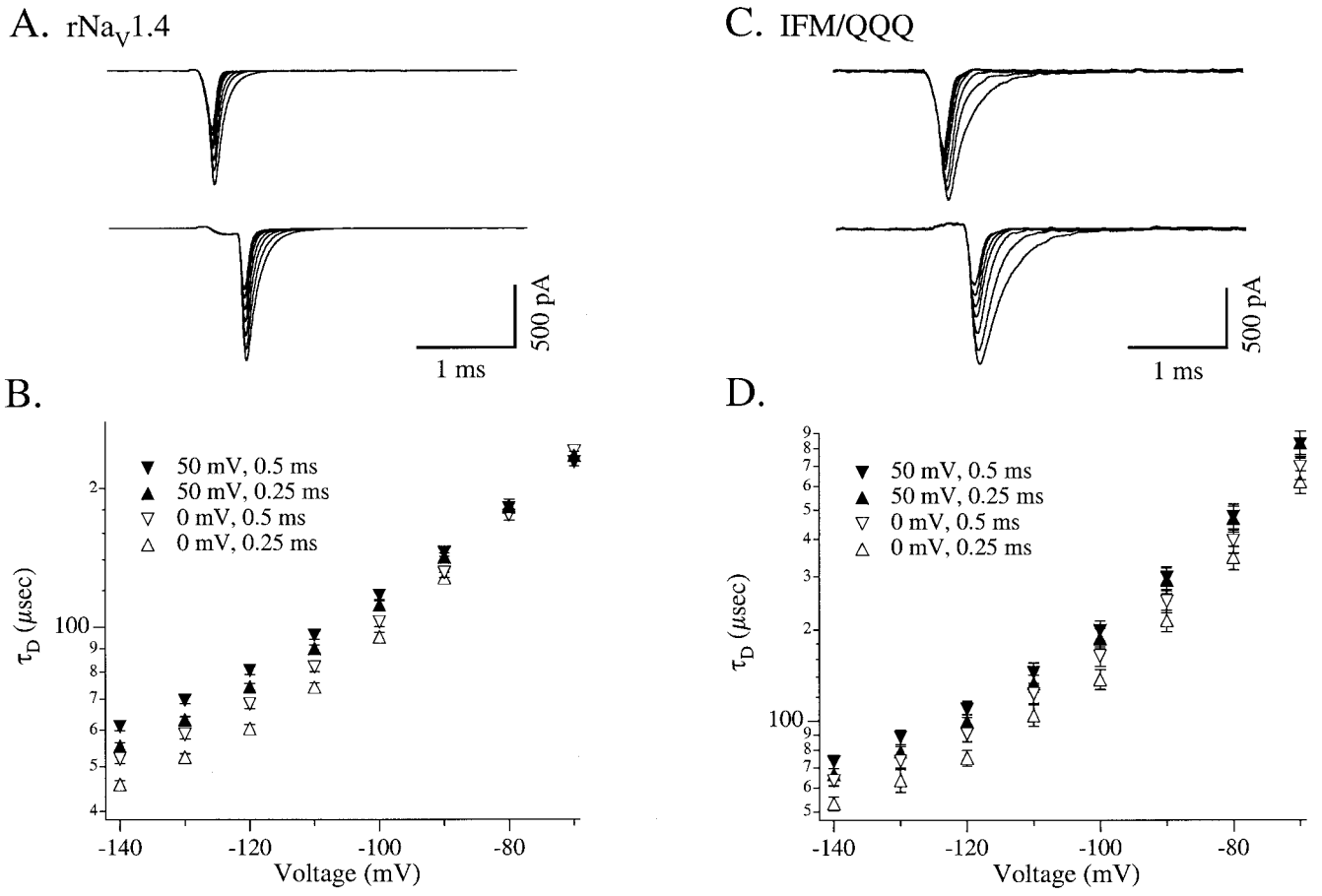

FIGURE 7 Voltage dependence of τ_D in rNa$_V$1.4 and IFM/QQQ. Tail currents are shown for rNa$_V$1.4 (*A*) and for IFM/QQQ (*C*) for the 0-mV, 0.25-ms protocol (*top record*) or the 50-mV, 0.5-ms protocol (*bottom record*) used to open channels. Voltage dependence of τ_D in rNa$_V$1.4 (*B*, $n = 32$) and in IFM/QQQ (*D*, $n = 17$) for each of four tail current protocols used; values represent mean ± SEM.

Fast inactivation is disrupted by R/Q substitution at specific residues in DIVS4

We found that most charge neutralizations in DIVS4 slowed entry into the fast-inactivated state. Charge neutralizations in DIVS4 have been used to assess the role in inactivation of the first residue in rNa$_V$1.4 or hNa$_V$1.4 (Chahine et al., 1994), the first and third residues in hNa$_V$1.5 (Chen et al., 1996), the second and third residues in rat brain IIA (Kontis and Goldin, 1997), or the two central residues in rNa$_V$1.2 (Kühn and Greef, 1999). Our results are generally very consistent with these studies, with a few minor differences. First, we observed in rNa$_V$1.4 that R3Q increased τ_h to an extent similar to that observed for R2Q, unlike in hNa$_V$1.5 (Chen et al., 1996). Second, we found that R4Q in rNa$_V$1.4 exhibited slightly steeper voltage dependence for τ_h than in rat brain IIA (Kontis and Goldin, 1997) and that fast inactivation was slowed by this mutation at voltages more positive than −40 mV. Our findings that charge neutralizations at R1–3 in DIVS4 slowed activation and entry into the fast-inactivated state are consistent with studies suggesting a role for these residues in the coupling of activation with fast inactivation (Chahine et al., 1994; Chen et al., 1996; Kontis and Goldin, 1997; Sheets et al., 1999; Horn et al., 2000).

Recovery from fast inactivation is regulated by the I-to-C transition

Sodium channels that enter the fast-inactivated state recover by deactivating (Kuo and Bean, 1994). We found that recovery rates for R/Q mutations in DIVS4 were predictable from recovery delay measurements. Neutralization of central charges in DIVS4 reduce charge immobilization and accelerate recovery (Kühn and Greef, 1999). These findings suggest that the I-to-C transition in DIVS4 regulates the recovery from fast inactivation.

The h_∞ curve was hyperpolarized for R1–5/Q compared to rNa$_V$1.4. Because we tested recovery over a voltage range from −190 mV to −90 mV, these mutations could possibly inactivate from the closed state at more depolarized interpulse voltages in the recovery protocol, an effect that would slow the rate at which channels become available.

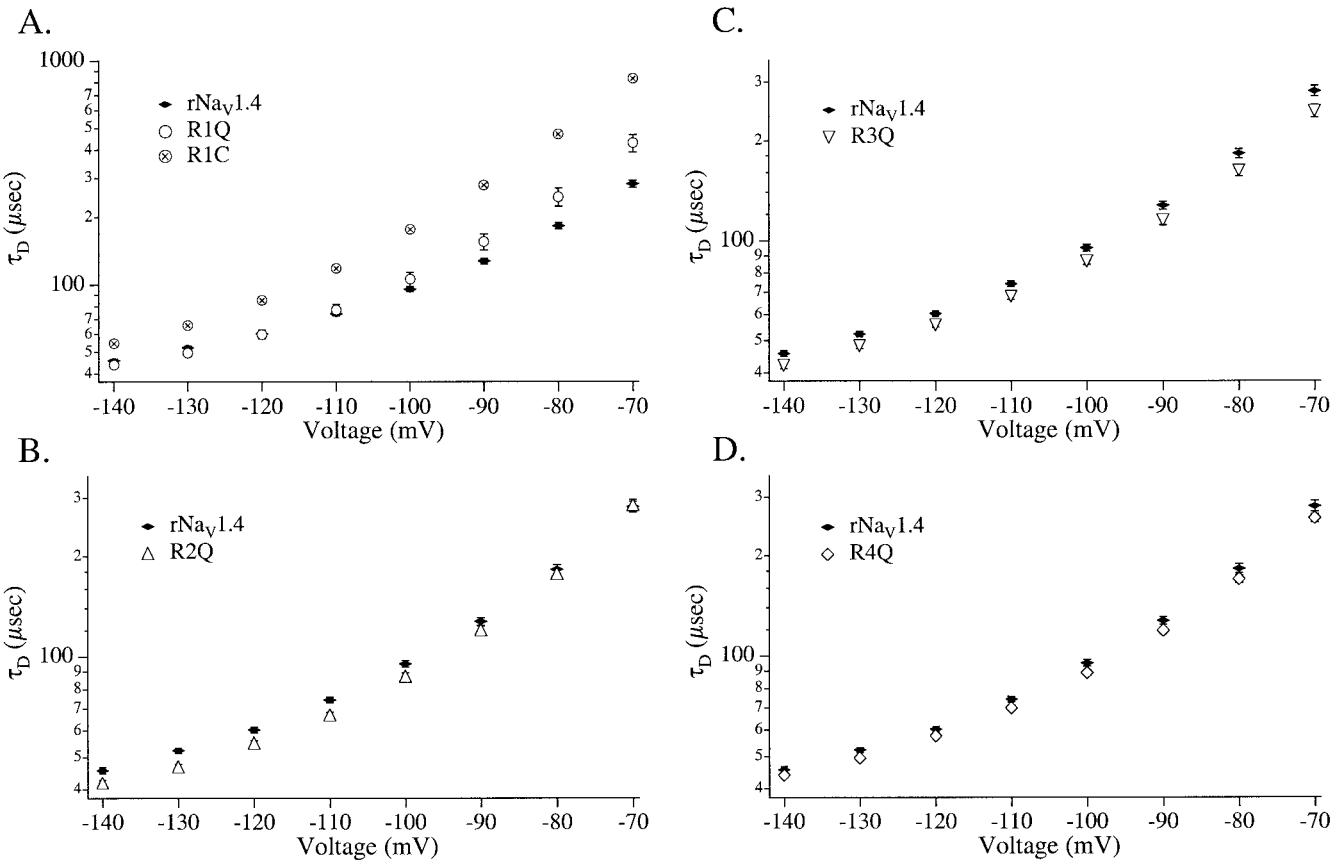

FIGURE 8 Voltage dependence of open state deactivation in rNaV1.4, R1C and R1–4/Q (*A*--*D*) with command hyperpolarizations following a depolarization to 0 mV for 0.25 ms to open channels. Values represent mean ± SEM; n = 31–56.

For example, we found that R2Q, R3Q, and R4Q produced progressively larger hyperpolarizing shifts in the h_∞ curve correlated with progressively longer recovery delays. One possible interpretation of longer recovery delay in R2–4/Q is that closed state inactivation occurs during recovery interpulses and slows the rate at which channels become available. However, recovery delay was slowed by R2–4/Q compared to $rNa_V1.4$ at voltages as negative as −190 mV, while effects of R2–4/Q on the h_∞ curve were similar to $rNa_V1.4$ at voltages of −140 mV or more negative. In addition, whereas R1Q and R5Q also hyperpolarized the h_∞ curve, both of these mutations abbreviated recovery delay. Thus, the effects of R/Q substitutions in DIVS4 on recovery delay are due to effects on the I-to-C transition, at least at more hyperpolarized voltages.

Deactivation in DIVS4 is not coupled to sodium channel activation

Our data suggest that differential effects of charge neutralizations in DIVS4 on deactivation from the open or inactivated state are independent from a coupling of activation to fast inactivation. We found that each of the R/Q mutations in DIVS4 produced a positive shift in $g(V_{1/2})$, decreased the apparent valence of activation, and/or increased the time to peak activation. These data are consistent with the findings from studies of other sodium channel isoforms in which glutamine was substituted for arginine residues in DIVS4 (Stühmer et al., 1989; Chen et al., 1996; Kontis and Goldin, 1997). We found that effects of R/Q mutations on the rate of activation were not always correlated with effects on deactivation kinetics. On one hand, R1Q slowed both activation and open-state deactivation. On the other hand, R2Q, R3Q, and R6Q each slowed activation while accelerating open-state deactivation. In these mutations, R1Q and R6Q abbreviated inactivated-state deactivation, whereas R2Q and R3Q slowed inactivated-state deactivation. Thus, although outer charges in DIVS4 have been previously demonstrated to couple activation with fast inactivation, effects of R/Q mutations in DIVS4 on activation parameters do not predict the effects of these mutations on deactivation from either the open or inactivated state.

Role for R1 in recovery from fast inactivation

We found that R1Q decreased the delay in the onset to recovery from fast inactivation, and increased the rate of

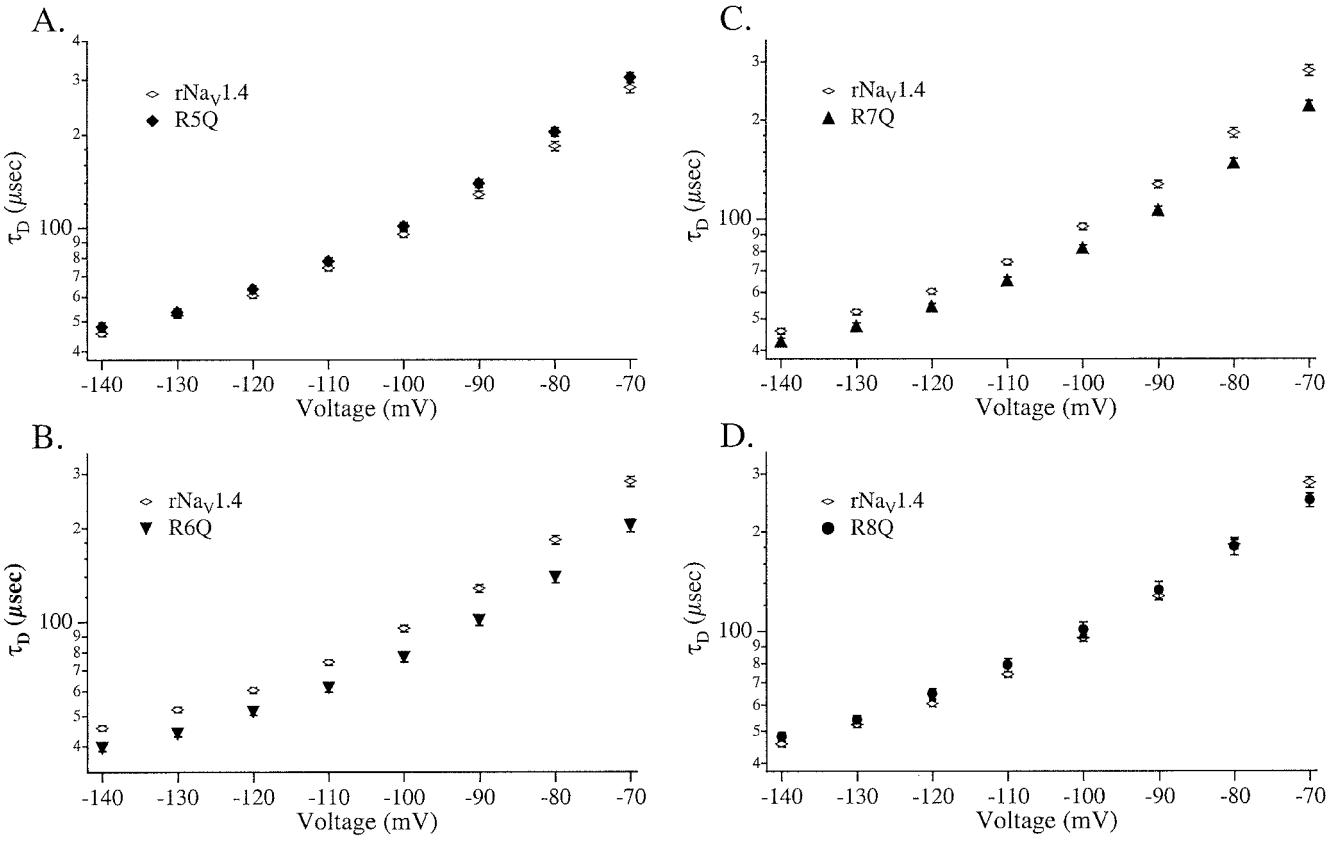

FIGURE 9 Voltage dependence of open-state deactivation in rNaV1.4 and in R5–8/Q (*A--D*) with command hyperpolarizations following a depolarization to 0 mV for 0.25 ms to open channels. Values represent mean ± SEM; $n = 29–48$.

recovery from fast inactivation. By contrast, charge substitution with R1K altered neither recovery delay nor rate. Similar effects on recovery have been noted with charge neutralizing mutations at this position in rNa$_V$1.4 and in hNa$_V$1.4 (Ji et al., 1996; Groome et al., 1999, 2000). Charge neutralizations at R1 in hNa$_V$1.4 or hNa$_V$1.5 are associated with a reduction in gating charge immobilization during fast inactivation (Cha et al., 1999; Sheets et al., 1999; Ruben et al., 1999). These findings suggest that neutralization of the outermost charge in DIVS4 accelerates the I-to-C transition as a result of a reduction in gating charge immobilization. Effects of charge neutralizations at R1 are consistent with a model for deactivation from the inactivated state in which voltage-dependent S4 translocation precedes a voltage-independent unbinding of the inactivation particle (Kuo and Bean, 1994; Kuo and Liao, 2000).

Role for central charges in recovery from fast inactivation

We found that recovery from fast inactivation was affected by other R/Q mutations of DIVS4 in a manner dependent upon the position relative to the center of the voltage sensor. For example, R5Q and R6Q decreased delay and accelerated recovery, with the magnitude of the effect on delay as R5Q > R6Q. The effect of R5Q to abbreviate recovery delay is consistent with the finding that neutralization of this residue decreases gating charge immobilization (Ruben et al., 1999). In contrast, neutralization of residues R2 to R4 on the N terminal side of center increased delay and slowed recovery, with an effect on delay as R4Q > R3Q > R2Q. Kühn and Greef (1999) found that the effect of R4H in rNa$_V$1.2 to slow recovery was a consequence of a slower return of immobilizable charge. Our finding that R4Q slowed recovery and increased recovery delay might be explained by a similar effect of this mutation.

In contrast to the effects of charge substitution at R1, we found that R4K and R5K produced effects on recovery delay and rate that were not similar to rNa$_V$1.4. Therefore, the contributions of individual residues during S4 translocation in the I-to-C transition may depend not only on charge content, but also on structural interactions of these arginine residues with amino acids in neighboring segments. Studies by Kontis and Goldin (1997) and Kontis et al. (1997) comparing charge neutralizing and charge substi-

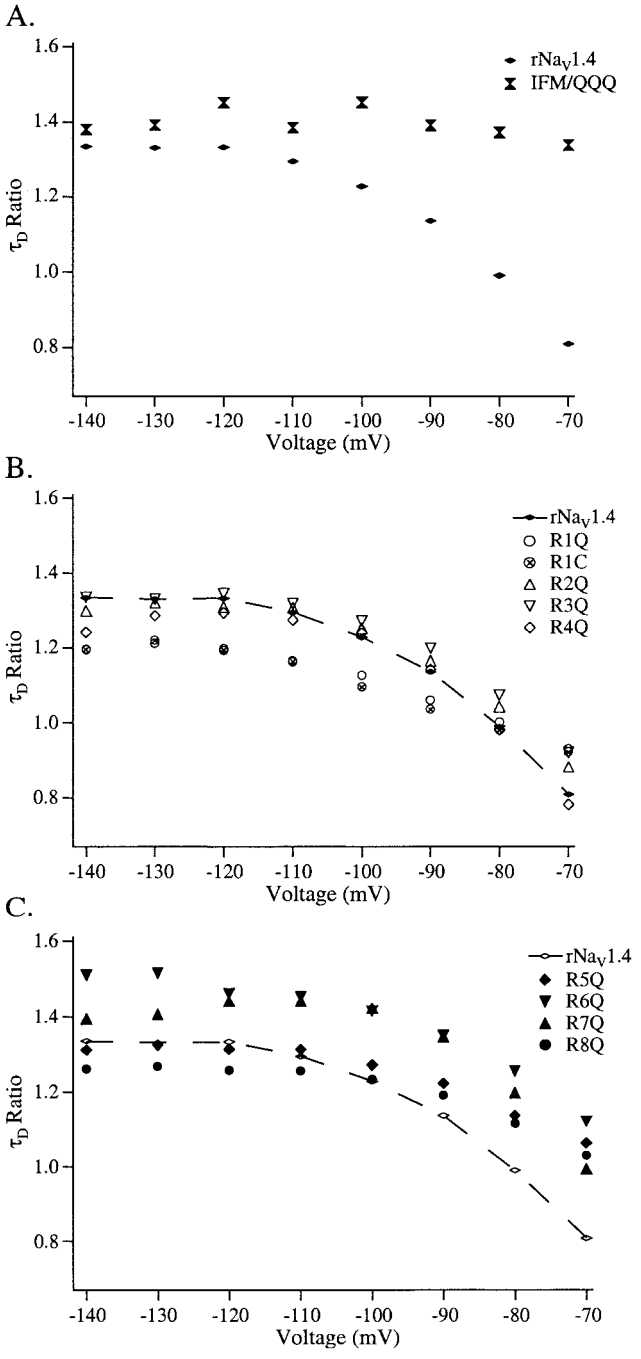

FIGURE 10 Voltage dependence of the effect of pulse duration and voltage on τ_D for $rNa_V1.4$, IFM/QQQ, and charge-neutralizing mutations in DIVS4. Magnitude of the effect was calculated as the ratio of τ_D for tail currents using the 50-mV depolarization, 0.5-ms protocol compared to τ_D for tail currents using the 0-mV depolarization, 0.25-ms protocol. Comparisons of τ_D for $rNa_V1.4$ to τ_D for IFM/QQQ (*A*), R1C and R1-R4/Q (*open symbols, B*), and R5-R8/Q (*closed symbols, C*) are shown. In (*B*) and (*C*) a dotted line is included with $rNa_V1.4$ for clarity. Values represent mean; $n = 29–56$.

tuting mutations of S4 segments in each of the four domains in $rNa_V1.2$ also suggest that structural interactions play a role in voltage sensor translocations.

The molecular basis for the allosteric effects of R/Q mutations in DIVS4 is uncertain without any detailed structural data about this region of the channel. Nonetheless, local structural interactions may be important determinants in the regulation of fast inactivation by DIVS4. For example, results from a study by Ji et al. (1996) suggest that DIVS3 and DIVS4 interact to regulate entry into and recovery from fast inactivation. In addition, Kühn and Greef (1999) postulated that negative countercharges could interact with the central arginine residues of DIVS4 to regulate the movement of the voltage sensor during inactivation and recovery, in a mechanism similar to the electrostatic interaction of residues in S2 and S4 segments of *Shaker* potassium channels (Papazian et al., 1995). Our data support a model in which an altered structure of the arginine moiety at either R4 or R5 disrupts the interaction of the charged residue with the local environment to impede (R4Q) or facilitate (R4K, R5Q, R5K) the movement of the voltage sensor into its hyperpolarized favored position during the I-to-C transition.

Role of fast inactivation in tail current decay

We used the IFM/QQQ mutation to determine the voltage range over which tail currents represent deactivation (Featherstone et al., 1998). Tail currents that decay completely in the absence of the IFM motif should represent deactivation, which we found to occur over a voltage range from −140 mV to −70 mV. We found that tail currents were slowed in IFM/QQQ compared to $rNa_V1.4$ over this voltage range. We also found that the τ_D ratio was voltage-dependent in $rNa_V1.4$, but not in IFM/QQQ. Our finding that removal of fast inactivation with mutagenesis-increased τ_D is similar to the finding by Cota and Armstrong (1989) that τ_D increased following enzymatic removal of fast inactivation. These authors interpreted the difference in τ_D (before and after exposure to papain) to represent the current decay due to fast inactivation. Although it has been shown that enzymatic removal of fast inactivation is not equivalent to removal of fast inactivation with mutagenesis of the IFM motif (Sheets et al. 2000), conclusions regarding the effects of charge-neutralizing mutations in DIVS4 on open-state deactivation must consider the relative effects of these mutations on fast inactivation and τ_D ratio.

If effects of mutations on deactivation were directly dependent on changes in fast inactivation, one would expect that rates of fast inactivation correlate to the rate of deactivation. Neutralizations at R1 do not follow this prediction. We found that while R1C and R1Q each slowed tail currents, effects of R1C were much greater. In contrast, each of these mutations produced identical effects on τ_h at 0 mV (R1Q = 2.1 ± 0.09 ms, R1C = 2.2 ± 0.08 ms). In addition, effects of R1C and R1Q on τ_D ratio were indistinguishable, and were less than $rNa_V1.4$ at voltages up to −80 mV. The differential effects of R1C and R1Q on tail current decay,

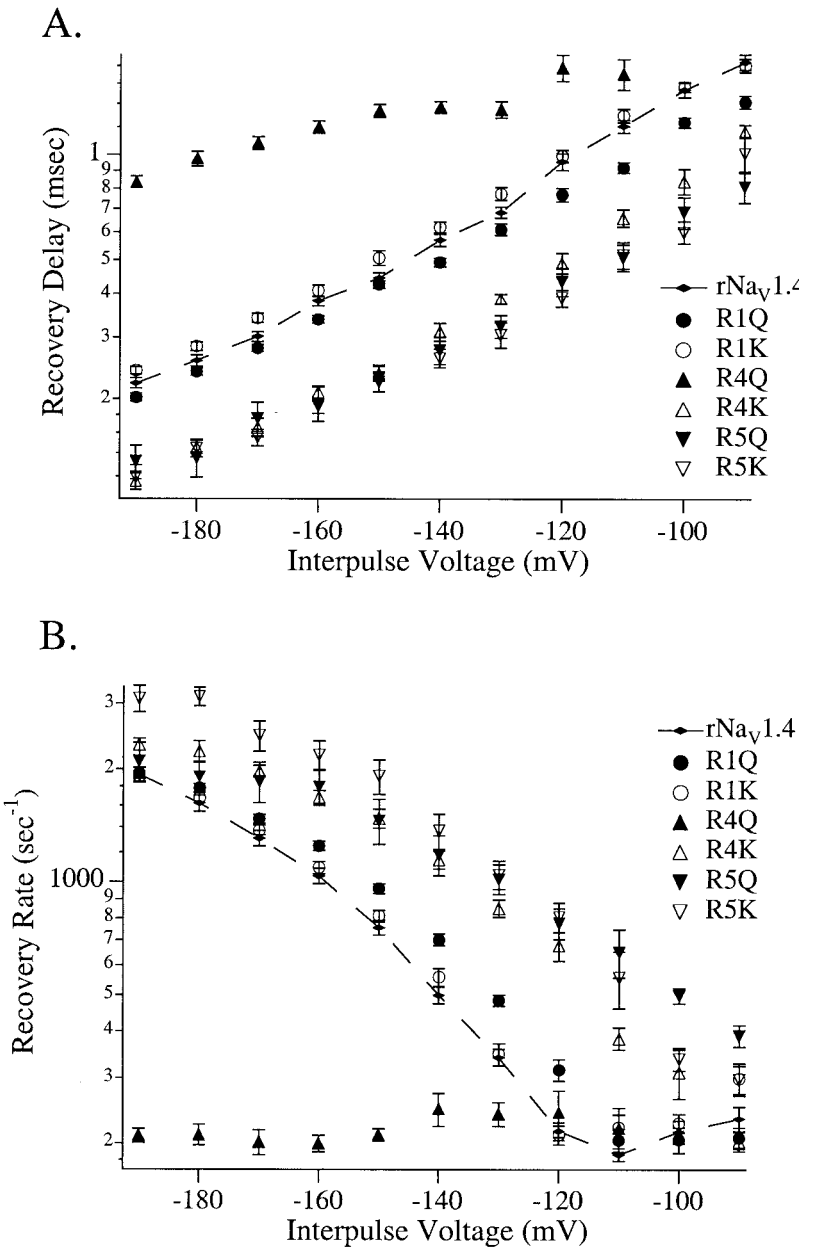

FIGURE 11 Comparison of charge neutralizing and charge substituting mutations at positions R1, R4 and R5 for recovery delay (*A*) or rate (*B*). In each graph a dotted line is included with rNa$_V$1.4, for clarity. Values represent mean ± SEM; n = 8–16 for charge-substituting mutations.

but identical effects on τ_h and τ_D ratio, suggest that slowing of tail currents with neutralization at R1 is due, at least in part, to a slowing of open-state deactivation. Neutralization at one of the central residues (R5Q) also increased τ_D and τ_h. The τ_D ratio for R5Q at depolarized commands was higher than rNa$_V$1.4. Thus, slowed fast-inactivation may have contributed to the effect of R5Q to prolong tail currents following short depolarizations.

Charge neutralizations at several residues in DIVS4 accelerated deactivation, in contrast to their effects on fast inactivation. For example, R2Q, R3Q, and R6Q slowed the rate of fast inactivation, but accelerated deactivation. R6Q and R7Q increased τ_D ratio compared to rNa$_V$1.4. If fast inactivation contributes to tail current decay in these mutations, the magnitude of the effects of these mutations to accelerate deactivation from the open state may be underestimated from tail current measurements. Taken together, these findings indicate that charge neutralizations in DIVS4 have differential effects on deactivation from the open state.

Role of R1 in open-state deactivation

Open-state deactivation kinetics are slowed by mutations of R1 in DIVS4 in the paramyotonia congenita mutations R1448C, R1448P, and R1448S (Ji et al., 1996; Bendahhou

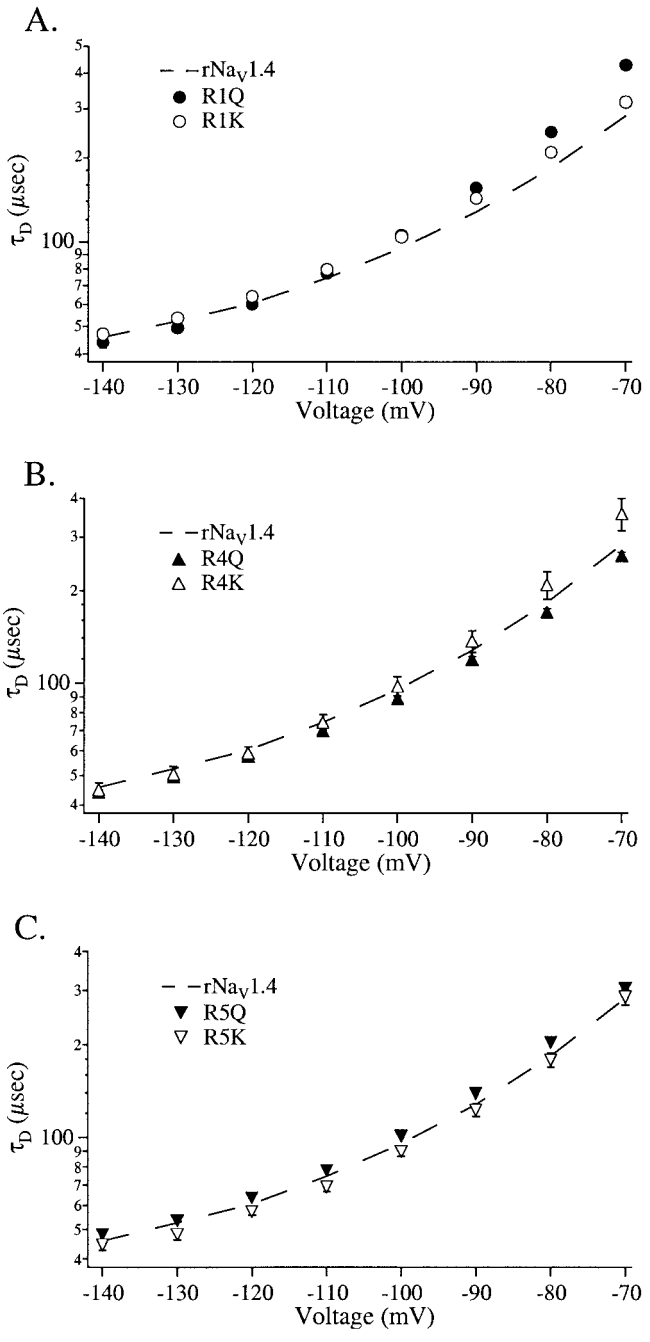

FIGURE 12 Comparison of charge neutralizing and charge substituting mutations at positions R1 (*A*), R4 (*B*), and R5 (*C*) for open-state deactivation using 0-mV, 0.25-ms depolarizations to open channels, followed by command hyperpolarizations. In each graph a dotted line is used to denote τ_D for $rNa_V1.4$, for clarity. Values represent mean ± SEM; $n = 16–40$ for charge-substituting mutations.

et al., 1999; Groome et al., 1999). Open-state deactivation is also slowed by charge neutralizations of the analogous residue in $rNa_V1.4$ (Featherstone et al., 1998; Groome et al., 2000). We compared the effects of charge-neutralizing (R1Q) and substituting (R1K) mutations at position R1 in $rNa_V1.4$. Deactivation was prolonged in R1Q to a greater extent than in R1K, suggesting that this residue influences deactivation gating with interaction of positive charge with the transmembrane electric field. In addition, the finding that substitution of cysteine for arginine at R1 prolonged tail currents to a greater extent than observed with glutamine substitution suggests that structural interactions of R1 with neighboring residues also influences the deactivation gating transition. This interpretation is consistent with the finding that several charge-neutralizing mutations at this residue associated with paramyotonia congenita differentially affect the O-to-C transition (Chahine et al., 1994; Featherstone et al., 1998).

Role of central charges in open-state deactivation

Neutralization of charge at R4 or R5 produced lesser effects on open-state deactivation than did R1Q. We found that R4Q accelerated deactivation, with charge substitution (R4K) resulting in a reversal of the deactivation profile. Thus, charge neutralization at R4 has a minor effect on open-state deactivation via an allosteric effect. R5Q slightly slowed open-state deactivation, with charge substitution (R5K) resulting in a deactivation profile more closely resembling $rNa_V1.4$. R5, like R1, may interact with the electrical field during open-state deactivation. However, the effect of R5Q to slow fast inactivation appears to account in part for the effect of this mutation to prolong tail current decay.

Open-state deactivation: domain-specific regulation

We have previously shown that neutralization of the outermost charge in DIII or DIV in hSkM1 slows deactivation, while neutralization of DI accelerates deactivation (Groome et al., 1999). These findings, and the observation that charge neutralizations in DIII and DIV cooperatively slow deactivation, motivated the present study to investigate each arginine residue in DIVS4. We found that open-state deactivation is regulated primarily by positive charge associated with the outermost arginine. Therefore, if DIVS4 is the first of the four voltage sensors to move during, and thus regulate, open-state deactivation, this movement is initiated primarily as a consequence of the charge associated with the outermost arginine. Kontis and Goldin (1997) found that neutralization of the second or fourth charged residue in DI and DII of $rNa_V1.2$ accelerated deactivation, neutralization at the fourth charged residue slowed deactivation in DIII, and neutralization at either the second or fourth charged residue in DIV was without effect. Taken together, these studies indicate that a limited number of arginine residues regulate sodium channel open-state deactivation.

We thank J. Repscher for help with experiments. We thank J. Abbruzzese and Y. Vilin for comments on a draft of this manuscript.

This work was supported by a Harvey Mudd College faculty research grant to J.G., and by Public Health Service Grant R01-NS29204 and a Research grant from the Muscular Dystrophy Association to P.R.

REFERENCES

Abbruzzese, J. L., E. Fujimoto, and P. C. Ruben. 1998. Differential effects on fast inactivation of domain IVS4 charge neutralizations. *Biophys. Abstr.* 74:401.

Aldrich, R. W., D. P. Corey, and C. F. Stevens. 1983. A reinterpretation of mammalian sodium channel gating based on single channel recording. *Nature.* 306:436–441.

Armstrong, C. M., and F. Bezanilla. 1977. Inactivation of the sodium channel. II. Gating current experiments. *J. Gen. Physiol.* 70:567–590.

Bendahhou, S., T. R. Cummins, H. Kwiecinski, S. G. Waxman, and L. J. Ptacek. 1999. Characterization of a new sodium channel mutation at arginine 1448 associated with moderate paramyotonia congenita in humans. *J. Physiol.* 518:337–344.

Cha, A., P. C. Ruben, A. L. George, Jr., E. Fujimoto, and F. Bezanilla. 1999. Voltage sensors in domains III and IV, but not I and II, are immobilized by Na^+ channel fast inactivation. *Neuron.* 22:73–87.

Chahine, M., A. L. George, Jr., M. Zhou, S. Ji, W. Sun, R. L. Barchi, and R. Horn. 1994. Sodium channel mutations in paramyotonia congenita uncouple inactivation from activation. *Neuron.* 12:281–294.

Chen, L-Q., V. Santarelli, R. Horn, and R. G. Kallen. 1996. A unique role for the S4 segment of domain 4 in the inactivation of sodium channels. *J. Gen. Physiol.* 108:549–556.

Cota, G., and C. M. Armstrong. 1989. Sodium channel gating in clonal pituitary cells. The inactivation step is not voltage dependent. *J. Gen. Physiol.* 94:213–232.

Featherstone, D. E., E. Fujimoto, and P. C. Ruben. 1998. A defect in skeletal muscle sodium channel deactivation exacerbates hyperexcitability in human paramyotonia congenita. *J. Physiol.* 506:627–638.

Groome, J. R., E. Fujimoto, A. L. George, Jr., and P. C. Ruben. 1999. Differential effects of homologous S4 mutations in human skeletal muscle sodium channels on deactivation gating from open and inactivated states. *J. Physiol.* 516:687–698.

Groome, J. R., E. Fujimoto, and P. C. Ruben. 2000. The delay in recovery from fast inactivation in skeletal muscle sodium channels is deactivation. *Cell. Mol. Neurobiol.* 20:521–527.

Groome, J. R., E. Fujimoto, L. Walter, and P. Ruben. 2001. Deactivation kinetics of skeletal muscle Na^+ channels are differentially affected by charge neutralizations in DIVS4. *Biophys. Abstr.* 80:233.

Ho, H. N., H. D. Hunt, R. M. Morton, J. K. Pullen, and L. R. Pease. 1989. Site-directed mutagenesis by overlap extension using the polymerase chain reaction. *Gene.* 77:51–59.

Hodgkin, A. L., and A. F. Huxley. 1952. A quantitative description of membrane current and its application to conduction and excitation in nerve. *J. Physiol.* 117:500–544.

Horn, R., S. Ding, and H. J. Gruber. 2000. Immobilizing the moving parts of voltage-gated ion channels. *J. Gen. Physiol.* 116:461–475.

Ji, S., A. L. George, Jr., R. Horn, and R. L. Barchi. 1996. Paramyotonia congenita mutations reveal different roles for segments S3 and S4 of domain D4 in hSkM1 sodium channel gating. *J. Gen. Physiol.* 107: 183–194.

Kellenberger, S., T. Scheuer, and W. A. Catterall. 1996. Movement of the Na^+ channel inactivation gate during inactivation. *J. Biol. Chem.* 271: 30971–30979.

Keynes, R. D., and H. Meves. 1993. Properties of the voltage sensor for the opening and closing of the sodium channels in the squid giant axon. *Proc. R. Soc. Lond. B.* 253:61–68.

Kontis, K. J., and A. L. Goldin. 1997. Sodium channel inactivation is altered by substitution of voltage sensor positive charges. *J. Gen. Physiol.* 110:403–413.

Kontis, K. J., A. Rounaghi, and A. L. Goldin. 1997. Sodium channel activation gating is affected by substitutions of voltage sensor positive charges in all four domains. *J. Gen. Physiol.* 110:391–401.

Kühn, F. J. P., and N. G. Greef. 1999. Movement of voltage sensor S4 in domain 4 is tightly coupled to sodium channel fast inactivation and gating charge immobilization. *J. Gen. Physiol.* 114:167–183.

Kuo, C-C., and B. P. Bean. 1994. Na^+ channels must deactivate to recover from inactivation. *Neuron.* 12:819–829.

Kuo, C-C., and S-Y. Liao. 2000. Facilitation of recovery from inactivation by external Na^+ and location of the activation gate in neuronal Na^+ channels. *J. Neurosci.* 20:5639–5646.

Mitrovic, N., A. L. George, and R. Horn. 2000. Role of domain 4 in sodium channel slow inactivation. *J. Gen. Physiol.* 115:707–717.

Noda, M., S. Shizimu, T. Tanabe, T. Takai, T. Kayano, T. Ikeda, H. Takahashi, Nakayama, Y. Kanaoka, N. Minamino, K. Kangawa, K. Matsuo, H. Raftery, M. Hirose, T. Inayama, H. Hayashida, T. Miyata, and S. Numa. 1984. Primary structure of *Electrophorus electricus* sodium channel deduced from cDNA sequence. *Nature.* 312:121–127.

Papazian, D. M., X. M. Shao, S-A. Seoh, A. F. Mock, Y. Huang, and D. H. Wainstock. 1995. Electrostatic interactions of S4 voltage sensor in *Shaker* K^+ channel. *Neuron.* 14:1–20.

Raman, I. M., and B. P. Bean. 2001. Inactivation and recovery of sodium currents in cerebellar Purkinje neurons: evidence for two mechanisms. *Biophys. J.* 80:729–737.

Rayner, M. D., J. G. Starkus, and P. C. Ruben. 1993. Hydration forces in ion channel gating. *Comments in Mol. Cell. Biophys.* 8:155–187.

Ruben, P., A. Cha, J. Abbruzzese, E. Fujimoto, and F. Bezanilla. 1999. DIVS4 mutations in rSkM1 and hSkM1 sodium channels uncouple charge immobilization from fast inactivation. *Biophys. Abstr.* 76:194.

Sheets, M. F., J. W. Kyle, and D. A. Hanck. 2000. The role of the putative inactivation lid in sodium channel gating current immobilization. *J. Gen. Physiol.* 115:609–619.

Sheets, M. F., J. W. Kyle, R. G. Kallen, and D. A. Hanck. 1999. The Na^+ channel voltage sensor associated with inactivation is localized to the external charged residues of domain IV, S4. *Biophys. J.* 77:747–757.

Stühmer, W., F. Conti, H. Suzuki, X. Wang, M. Noda, N. Yahagi, H. Kubo, and S. Numa. 1989. Structural parts involved in activation and inactivation of the sodium channel. *Nature.* 339:597–604.

Trimmer, J. S., S. S. Coopoerman, S. A. Tomiko, J. Zhou, S. M. Crean, M. B. Boyle, R. G. Kallen, Z. Sheng, R. L. Barchi, F. J. Sigworth, R. H. Goodman, W. S. Agnew, and G. Mandel. 1989. Primary structure and functional expression of a mammalian skeletal muscle sodium channel. *Neuron.* 3:33–49.

Vassilev, P. M., T. Scheuer, and W. A. Catterall. 1988. Identification of an intracellular peptide segment involved in sodium channel inactivation. *Science.* 241:1658–1661.

West, J. W., D. E. Patton, T. Schuere, T. Wang, A. L. Goldin, and W. A. Catterall. 1992. A cluster of hydrophobic residues required for fast Na^+ channel inactivation. *Proc. Natl. Acad. Sci. U.S.A.* 89:10910–10914.

Yang, N., A. L. George, and R. Horn. 1996. Molecular basis of charge movement in voltage-gated sodium channels. *Neuron.* 16:113–122.

Yang, N., and R. Horn. 1995. Evidence for voltage-dependent movement in sodium channels. *Neuron.* 15:213–216.